



Nuclear modification factor of light neutral-meson spectra up to high transverse momentum in p–Pb collisions at $\sqrt{s_{NN}} = 8.16$ TeV



ALICE Collaboration*

ARTICLE INFO

Article history:

Received 17 November 2021

Received in revised form 27 January 2022

Accepted 28 January 2022

Available online 1 February 2022

Editor: M. Doser

ABSTRACT

Neutral pion (π^0) and η meson production cross sections were measured up to unprecedentedly high transverse momenta (p_T) in p–Pb collisions at $\sqrt{s_{NN}} = 8.16$ TeV. The mesons were reconstructed via their two-photon decay channel in the rapidity interval $-1.3 < y < 0.3$ in the ranges of $0.4 < p_T < 200$ GeV/c and $1.0 < p_T < 50$ GeV/c, respectively. The respective nuclear modification factor (R_{pPb}) is presented for p_T up to of 200 and 30 GeV/c, where the former was achieved by extending the π^0 measurement in pp collisions at $\sqrt{s} = 8$ TeV using the merged cluster technique. The values of R_{pPb} are below unity for $p_T < 10$ GeV/c, while they are consistent with unity for $p_T > 10$ GeV/c, leaving essentially no room for final state energy loss. The new data provide strong constraints for nuclear parton distribution and fragmentation functions over a broad kinematic range and are compared to model predictions as well as previous results at $\sqrt{s_{NN}} = 5.02$ TeV.

© 2022 European Organization for Nuclear Research. Published by Elsevier B.V. This is an open access article under the CC BY license (<http://creativecommons.org/licenses/by/4.0/>). Funded by SCOAP³.

1. Introduction

Measurements of identified hadron spectra in high-energy proton–proton (pp) collisions are well suited to constrain perturbative predictions from Quantum Chromodynamics (QCD) [1]. At large momentum transfer (Q^2) one relies in these perturbative QCD (pQCD) calculations on the factorization of computable short-range parton scattering processes such as quark–quark, quark–gluon and gluon–gluon scatterings from long-range properties of QCD that need experimental input. These non-perturbative properties are typically modeled by parton distribution functions (PDFs), which describe the fractional-momentum (x) distributions of quarks and gluons within the proton, and fragmentation functions (FFs), which describe the fractional-momentum (z) distribution of quarks or gluons for hadrons of certain species.

In high-energy proton–nucleus (p–A) collisions, nuclear effects are expected to significantly affect particle production, in particular at small x [2]. Previous measurements of neutral pions and charged hadrons in p–Pb collisions at $\sqrt{s_{NN}} = 5.02$ TeV at the LHC [3–6] indeed revealed distinct deviations from binary-scaled pp collisions, confirming earlier results from deuteron–gold collisions at $\sqrt{s_{NN}} = 0.2$ TeV at RHIC [7,8]. The modification at low p_T (~ 1 GeV/c), which is commonly attributed to nuclear shadowing, can be parameterized by nuclear parton distribution functions (nPDFs) [9,10]. However, the high parton densities reached at low p_T (x as small as $\sim 5 \cdot 10^{-4}$) make the Color Glass Con-

densate (CGC) framework [11] applicable which predicts strong particle suppression due to saturation of the parton phase space in nuclei [12]. Recently, also parton energy loss in cold nuclear matter was shown [13] to lead to suppressed particle yields at low p_T , while the previously observed collective effects in small systems [14–16] also imply partonic rescatterings in hot nuclear matter to play a role [17,18].

In this letter, the nuclear modification of particle yields is quantified by

$$R_{pPb} = \frac{1}{A_{Pb}} \frac{d^2\sigma_{pPb}}{dp_T dy} \bigg/ \frac{d^2\sigma_{pp}}{dp_T dy}, \quad (1)$$

where $A_{Pb} = 208$ is the nuclear mass number of lead and $d^2\sigma/(dp_T dy)$ are the π^0 or η meson cross sections measured in p–Pb collisions at $\sqrt{s_{NN}} = 8.16$ TeV and in the corresponding pp reference system at $\sqrt{s} = 8$ TeV. The new data constrain nPDFs and FFs over a large range in x , and Q^2 , including the center-of-mass energy dependence based on comparisons to lower-energy data [6].

2. Experimental setup

The neutral mesons were reconstructed via their two-photon decay channels $\pi^0(\eta) \rightarrow \gamma\gamma$ using different reconstruction techniques provided by the various subdetector systems of ALICE [19, 20]. Photons are either reconstructed using the Electromagnetic Calorimeter (EMCal), the Photon Spectrometer (PHOS) or via the Photon Conversion Method (PCM). The latter uses e^+e^- pairs from

* E-mail address: alice-publications@cern.ch.

Table 1

Trigger rejection factor RF and total integrated luminosities based on the individual samples for the different reconstruction methods and triggers in pp collisions at $\sqrt{s} = 8$ TeV and p-Pb collisions at $\sqrt{s_{NN}} = 8.16$ TeV. The uncertainty associated with the determination of the MB cross section of 1.9% for p-Pb and 2.6% for pp is not included. The value in brackets corresponds to the high luminosity minimum bias data sample where TPC tracking is not available.

| System/Trigger | RF | \mathcal{L}_{int} (nb $^{-1}$) | | | |
|-----------------|------------------------------|--|---------|-------|-------|
| | | (m)EMC | PCM-EMC | PCM | PHOS |
| p-Pb | | | | | |
| MB | – | 0.018(0.041) | 0.018 | 0.022 | 0.036 |
| EMCal L1 (low) | 288 ± 8 | 0.206 | 0.081 | – | – |
| EMCal L1 (high) | 991 ± 29 | 5.67 | 1.42 | – | – |
| PHOS L0 | $(1.66 \pm 0.02) \cdot 10^3$ | – | – | – | 1.68 |
| PHOS L1 | $(1.55 \pm 0.04) \cdot 10^4$ | – | – | – | 6.42 |
| pp | | | | | |
| MB | – | 1.94 | 1.94 | 2.17 | 1.25 |
| EMCal/PHOS L0 | 64.6 ± 1.0 | 39.4 | 39.4 | – | 136 |
| EMCal L1 | $(1.47 \pm 0.06) \cdot 10^4$ | 606 | 606 | – | – |

conversions, which are reconstructed from tracks measured in the Inner Tracking System (ITS) [21] and the Time Projection Chamber (TPC) [21] at $|\eta| < 0.9$ inside a solenoidal magnetic field of $B = 0.5$ T. The EMCal [22,23] is a lead-scintillator sampling electromagnetic calorimeter at a radial distance of 4.28 m from the interaction point (IP) covering $\Delta\phi = 100^\circ$ in azimuth for $|\eta| < 0.7$ in pseudorapidity during the 2012 pp data taking period. During the p-Pb data taking in 2016, additional modules [23] were available that extended the coverage to $\Delta\phi = 107^\circ$ for $|\eta| < 0.7$ and added $\Delta\phi = 60^\circ$ opposite in azimuth for $0.22 < |\eta| < 0.7$. The calorimeter provides an energy resolution of $\sigma_E/E = 4.8\%/E \oplus 11.3\%/\sqrt{E} \oplus 1.7\%$, with E in units of GeV. In its full configuration, it consists of a total of 18240 cells of transverse size 6×6 cm 2 each. The PHOS [24] is a lead tungstate electromagnetic calorimeter with 12544 channels at a distance of 4.6 m from the IP, covering $\Delta\phi = 70^\circ$ and $|\eta| < 0.12$. Its high light yield combined with its cell size being only slightly larger than the Molière radius of 2 cm results in an energy resolution of $\sigma_E/E = 1.8\%/E \oplus 3.3\%/\sqrt{E} \oplus 1.1\%$.

3. Data samples and event selection

The p-Pb data at $\sqrt{s_{NN}} = 8.16$ TeV were recorded in 2016. Equal magnetic rigidity for proton and Pb beams in the LHC resulted in a rapidity shift of $\Delta y_{NN} = 0.465$ in the direction of the proton beam between the nucleon-nucleon center-of-mass and the laboratory reference system. The minimum bias (MB) event trigger required a coincidence at Level 0 (L0) of signals issued by the VOA and VOC detectors, which are two arrays of 32 scintillator tiles each covering full azimuth at $2.8 < \eta < 5.1$ and $-3.7 < \eta < -1.7$, respectively [25]. Additional triggers at L0 required an energy deposit above 2 GeV for EMCal and 4 GeV for PHOS, in 4×4 adjacent cells in coincidence with the MB trigger. Based on the L0 preselection, further hardware Level 1 triggers were issued, two for the EMCal with energy thresholds at 5.5 GeV and 8 GeV and one for the PHOS at 7 GeV. To account for the yield enhancement of the event triggers, the trigger rejection factors (RF) for the EMCal triggers were estimated through an error function fit to the ratio of the cluster energy spectra in their plateau regions above the respective trigger thresholds. A similar procedure was performed for the PHOS triggers, where RF is determined on the ratio of the corrected π^0 meson spectra instead. The trigger rejection factors from these fits are given in Table 1 for all event triggers. For the high threshold triggers, RF is obtained from the product $RF_{\text{EMCal-L1low/MB}} \cdot RF_{\text{EMCal-L1high/low}}$ or $RF_{\text{PHOS-L0/MB}} \cdot RF_{\text{PHOS-L1/L0}}$. Uncertainties on RF are given as combined statistical and systematic uncertainties where the latter part was determined via variations of the low E fit range. The integrated luminosities (\mathcal{L}_{int}) of each trigger sample and for each reconstruction method were calculated

based on the MB cross section of $\sigma_{\text{MB}} = (2.09(2.10) \pm 0.04)$ b for the p-Pb (Pb-p) collisions [26] and the respective RF values as $\mathcal{L}_{\text{int}} = RF \times N_{\text{events}}/\sigma_{\text{MB}}$ and are listed in Table 1. For PCM-EMC lower integrated luminosities are reported due to the lack of TPC readout in two thirds of the triggered data. The pp collision data set at a center-of-mass energy of $\sqrt{s} = 8$ TeV used in this analysis was recorded in 2012 and the respective integrated luminosities and RF values are listed in Table 1.

4. Analysis

Reconstructed tracks were used to determine the primary vertex of the collision, which was required to be within 10 cm from the nominal IP position along the beam direction. Pileup events ($\sim 1.5\%$ in pp) containing multiple collisions within a 300 ns window were rejected if more than one primary vertex was reconstructed from SPD hits or if the number of SPD clusters was not correlated with the number of track candidates. The photon and meson reconstruction methods are analogous to those described in Refs. [6,27]. To achieve an optimal uncertainty cancellation on R_{ppb} , the meson analyses were performed simultaneously for the p-Pb and pp data sets using identical methods and selections, where possible.

Photon reconstruction in the EMCal (PHOS) is based on grouping adjacent cells, with energy deposits above $E_{\text{cell}}^{\text{min}} = 100$ (20) MeV, into clusters starting with a seed cell of $E_{\text{cell}}^{\text{seed}} > 500$ (50) MeV. The thresholds for PHOS are lower due to its better energy resolution and finer granularity. Photon candidates in the EMCal were required to have $|\eta_\gamma| < 0.67$ and a minimum of two cells in the cluster ($N_{\text{cell}}^{\text{cls}} \geq 2$). In addition, clusters are required to have a primarily round shape by restricting the cluster elongation (σ_{long}^2 [28]) to values between 0.1 and 0.5. The elongation σ_{long}^2 is defined as

$$\sigma_{\text{long}}^2 = \frac{1}{2} \left[\sigma_{\varphi\varphi}^2 + \sigma_{\eta\eta}^2 + \sqrt{(\sigma_{\varphi\varphi}^2 - \sigma_{\eta\eta}^2)^2 + 4\sigma_{\varphi\eta}^4} \right], \quad (2)$$

where the values of $\sigma_{ab}^2 = \langle ab \rangle - \langle a \rangle \langle b \rangle$ and $\langle a \rangle = (w_{\text{tot}})^{-1} \sum w_i a_i$ are based on the weighted cell energy compared to the cluster energy and in relative η and ϕ direction to the seed cell of the cluster. The weighting is logarithmic with $w_i = \max(0, 4.5 + \log(E_i/E_{\text{clus}}))$ where the sum of all w_i equals w_{tot} [28]. Small values of σ_{long}^2 denote clusters with a round shape that are primarily of photonic origin, while large values of σ_{long}^2 describe elongated clusters, which are primarily from hadronic sources or from overlapping showers.

In PHOS, $|\eta_\gamma| < 0.12$ was required and the criteria $\sigma_{\text{long}}^2 > 0.1$ and $N_{\text{cell}}^{\text{cls}} \geq 3$ were only applied to clusters with $E > 2$ GeV. Hadron

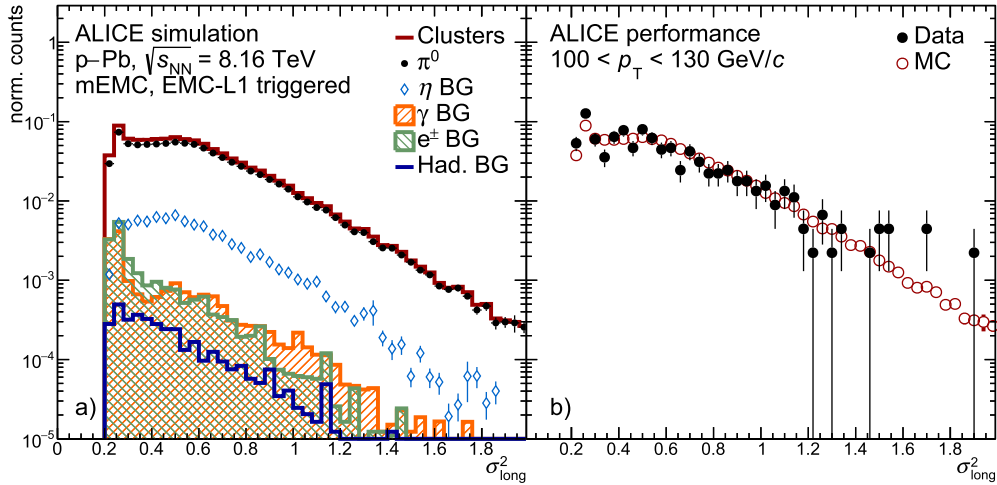


Fig. 1. Shower shape distribution for the elongation σ_{long}^2 in PYTHIA 8 Monte Carlo simulations a) showing the various contributions to the full cluster sample for a high p_T example interval and b) compared to the σ_{long}^2 distribution in data in the same p_T interval.

and electron contamination of the photon clusters in the EMCal was removed if an associated track was found with $E/p_{\text{track}} < 1.75$. The suppression of false matches with the E/p veto increased the photon efficiency by up to 50% at high p_T with respect to previous measurements [6,27]. Corrections for the non-linear energy response of the calorimeters were applied to the cluster energy. For the EMCal the correction was obtained from electron test beam data and from laboratory-based measurements of the low-gain shapers in the front-end electronics. The correction is sizeable only at low E (6% at 1 GeV) and at high E (14% at 200 GeV). It includes a residual relative energy-and-position correction, which is applied on simulated EMCal clusters to match the π^0 peak position in data. An improved description of the EMCal cluster properties in simulations was achieved by introducing a cross talk emulation within the same EMCal readout card as described in Ref. [29]. The resulting agreement of the π^0 mass peak position is better than 0.3% between data and simulation. For the PHOS, the energy non-linearity was corrected by fixing the reconstructed π^0 mass to the nominal PDG value [30].

Photon conversions were reconstructed by combining oppositely charged tracks, originating from a common vertex up to a radius of 180 cm, through a secondary vertex finder. Only tracks with a TPC dE/dx within -3σ and $+4\sigma$ of the expected values for electrons were accepted, where σ is the dE/dx resolution. Additionally, tracks with $p > 0.4$ GeV/c and dE/dx up to 1σ above the expected value for pions were rejected. For tracks with $p > 3.5$ GeV/c, this was loosened to 0.5σ . The photon conversion selection criteria were further optimized with respect to previous measurements [27,31] to yield about 10% better efficiency at similar purity.

An invariant mass ($m_{\gamma\gamma}$) technique was used for the reconstruction of neutral pions and η mesons. For this, $m_{\gamma\gamma}$ was calculated for all possible combinations of photon candidates per event taking either both photons reconstructed by the same method (called PCM, EMC, and PHOS), or one photon reconstructed with PCM and one with EMC (called PCM-EMC). The invariant mass distributions were calculated in p_T intervals of the meson candidates (examples are shown in Ref. [32]). For each interval, the combinatorial background, obtained from event mixing, and residual correlated background were subtracted (see Ref. [32]). The remaining distributions were then integrated in $\sim 3\sigma$ around the fitted mass peak position to determine the raw yields.

Neutral pions with $p_T > 16$ GeV/c were measured with the merged-cluster (mEMC) method [31], which exploits single clusters in the EMCal that result from overlapping energy deposits of

both decay photons in the same cluster due to the small opening angle for large pion momentum. The elongation ($\sigma_{\text{long}}^2 > 0.27$) of clusters with $p_T > 16$ GeV/c was used to discriminate between single-photon ($\sigma_{\text{long}}^2 \approx 0.25$) and merged-photon clusters. The σ_{long}^2 distribution was obtained in p_T -intervals of the clusters and the integrated counts above 0.27 were used as raw π^0 candidate yields. An exemplary σ_{long}^2 distribution at high p_T is shown in Fig. 1a in simulation, broken up into the individual contributions to the full cluster sample. Fig. 1b shows a comparison between the data and simulation σ_{long}^2 distributions, highlighting their good agreement within uncertainties. The resulting π^0 purity is between 81–87% decreasing with p_T in p-Pb and 83–89% in pp collisions. It was determined via PYTHIA 8 [33] simulations with additional data-driven corrections, which increase the relative fractions of prompt photons by 1–3% and of η mesons by 2%. POWHEG-Box [34,35] simulations were used to determine an additional purity correction for electrons from weak decays of up to 3%.

Correction factors for reconstruction efficiency and kinematic acceptance (see Ref. [32]) were obtained from simulations of the detector response with GEANT3 [36] using DPMJET [37] and PYTHIA 8 [33] as event generators. The correction factors for secondary π^0 from long-lived strange hadron decays were obtained from a particle-decay simulation based on measured spectra and are dominated by contributions from K_S^0 and Λ decays [27,38]. They amount to about 1–6% and decrease with p_T . For the PCM method, an additional correction for out-of-bunch pileup of 7 to 15% decreasing with p_T was applied.

The spectra were normalized by the integrated luminosities of each trigger sample and meson reconstruction method as listed in Table 1.

The systematic uncertainties on the π^0 (η) cross sections contain contributions from the yield extraction of 1–10% (2–20%) depending on the reconstruction method and p_T . Further contributions from the imperfect description of the selection variables in the simulation amount to 1–4% (1–6%), while the p_T -independent material-budget uncertainties are 4.5% per PCM photon, 2.8% per EMCal photon and 2% per PHOS photon. Uncertainties arising from the out-of-bunch pileup determination reach 3–5% and global uncertainties on the trigger rejection factors are 2–3% [32]. For the mEMC analysis, the largest systematic uncertainty arises from the shower overlaps in jets, which depend on the jet fragmentation and affect the π^0 energy resolution in the EMCal. This uncertainty was estimated as 7–10%, obtained from varying the particle overlaps within clusters. The total uncertainties on the π^0 (η) cross

Table 2

Summary of relative systematic uncertainties in percent for selected p_T intervals for the π^0 and η meson cross sections $\sigma_{p\text{-Pb}}$ and nuclear modification factors $R_{p\text{Pb}}$. The statistical uncertainties are given in addition to the total systematic uncertainties for each bin. The combined statistical and systematic uncertainties, obtained by applying the BLUE method [39,40], are also listed for all reconstruction methods available in the given p_T bin, considering the uncertainty correlations for the different methods. The uncertainty from the σ_{MB} determination of 1.9%, see Ref. [26], is independent of the reported measurements and is separately indicated in the figures.

| Source | | $\sigma_{p\text{-Pb}}^{\pi^0}$ | | | | $R_{p\text{Pb}}^{\pi^0}$ | | | | $\sigma_{p\text{-Pb}}^{\eta}$ | | | $R_{p\text{Pb}}^{\eta}$ | | | $\eta/\pi^0_{p\text{-Pb}}$ | | |
|-------------------------------|------------------------|--------------------------------|-----|-----|------|--------------------------|-----|------|------|-------------------------------|------|------|-------------------------|------|------|----------------------------|------|------|
| p_T (GeV/c) | | 1.6 | 5.5 | 17 | 115 | 1.6 | 5.5 | 17 | 115 | 2.75 | 7 | 22.5 | 2.75 | 7 | 22.5 | 2.75 | 7 | 22.5 |
| PCM | photon reco. | 10.7 | 9.1 | - | - | 0.7 | 1.5 | - | - | 9.5 | 10.5 | - | 2.0 | 3.0 | - | 2.7 | 4.6 | - |
| | meson reco. | 6.8 | 6.3 | - | - | 2.6 | 7.0 | - | - | 4.0 | 5.1 | - | 4.6 | 6.3 | - | 3.9 | 5.2 | - |
| | pileup | 5.5 | 3.3 | - | - | 5.9 | 6.3 | - | - | 4.9 | 4.1 | - | 6.1 | 6.1 | - | 2.6 | 1.9 | - |
| | stat. uncertainty | 2.2 | 6.7 | - | - | 3.0 | 9.2 | - | - | 12.0 | 25.9 | - | 18.7 | 37.3 | - | 12.9 | 25.9 | - |
| PCM-EMC | PCM photon reco. | 4.7 | 5.5 | 5.0 | - | 1.3 | 3.5 | 3.3 | - | 7.5 | 7.3 | 8.1 | 5.0 | 5.5 | 6.2 | 6.0 | 4.5 | 7.8 |
| | γ cluster reco. | 3.5 | 3.8 | 4.4 | - | 1.8 | 2.1 | 3.8 | - | 4.8 | 5.1 | 6.5 | 2.9 | 3.3 | 9.6 | 3.6 | 3.8 | 5.0 |
| | meson reco. | 2.4 | 1.0 | 1.5 | - | 2.9 | 2.3 | 2.2 | - | 3.3 | 4.7 | 14.4 | 5.5 | 5.4 | 8.3 | 3.7 | 6.3 | 14.4 |
| | trigger and efficiency | 1.0 | 1.0 | 3.0 | - | 0.5 | 3.2 | 4.9 | - | 1.0 | 2.0 | 3.0 | 0.2 | 3.2 | 4.9 | 1.4 | 1.4 | 1.4 |
| | stat. uncertainty | 2.2 | 3.7 | 3.6 | - | 2.6 | 5.7 | 5.3 | - | 14.2 | 11.4 | 16.4 | 0.0 | 0.0 | 0.0 | 14.1 | 14.0 | 12.5 |
| EMC | γ cluster reco. | 7.2 | 5.9 | 7.1 | - | 4.8 | 2.7 | 4.3 | - | 9.5 | 8.5 | 9.5 | 7.0 | 6.6 | 8.2 | 7.3 | 6.9 | 8.6 |
| | meson reco. | 3.5 | 4.1 | 7.3 | - | 5.1 | 4.7 | 7.0 | - | 23.7 | 7.3 | 3.0 | 29.4 | 8.3 | 4.8 | 23.9 | 7.9 | 8.6 |
| | trigger and efficiency | 2.3 | 2.4 | 4.1 | - | 1.7 | 1.7 | 4.5 | - | 2.3 | 3.0 | 3.8 | 2.6 | 2.6 | 5.1 | 2.0 | 2.5 | 2.5 |
| | stat. uncertainty | 3.1 | 2.0 | 4.2 | - | 4.4 | 3.1 | 5.3 | - | 20.8 | 7.9 | 6.9 | 23.9 | 15.4 | 27.8 | 20.9 | 8.1 | 12.5 |
| PHOS | γ cluster reco. | 3.2 | 3.7 | 3.8 | - | 2.0 | 2.0 | 2.0 | - | 4.1 | 4.2 | 4.2 | - | - | - | 0.0 | 0.0 | 0.0 |
| | meson reco. | 2.1 | 2.9 | 4.9 | - | 3.5 | 3.3 | 5.2 | - | 18.0 | 4.5 | 7.0 | - | - | - | 34.6 | 7.9 | 12.4 |
| | trigger and efficiency | 2.8 | 2.8 | 3.4 | - | 7.4 | 7.4 | 14.6 | - | 1.6 | 2.5 | 2.5 | - | - | - | 1.0 | 1.0 | 1.0 |
| | stat. uncertainty | 1.1 | 3.1 | 3.6 | - | 5.4 | 6.9 | 11.7 | - | 29.7 | 6.5 | 15.9 | - | - | - | 17.5 | 5.8 | 12.9 |
| mEMC | meson PID | - | - | 5.4 | 5.8 | - | - | 2.3 | 3.6 | - | - | - | - | - | - | - | - | - |
| | cluster reco. | - | - | 8.3 | 9.5 | - | - | 1.0 | 1.0 | - | - | - | - | - | - | - | - | - |
| | trigger and efficiency | - | - | 4.1 | 4.1 | - | - | 3.8 | 3.8 | - | - | - | - | - | - | - | - | - |
| | stat. uncertainty | - | - | 2.4 | 5.7 | - | - | 2.7 | 10.8 | - | - | - | - | - | - | - | - | - |
| combined syst. uncert. | | 3.6 | 3.9 | 4.9 | 11.9 | 2.7 | 2.9 | 2.9 | 5.4 | 5.6 | 5.3 | 6.1 | 5.9 | 6.8 | 11.5 | 8.6 | 4.5 | 8.2 |
| combined stat. uncert. | | 1.0 | 1.8 | 2.2 | 5.7 | 1.8 | 2.7 | 2.2 | 10.8 | 8.6 | 4.5 | 8.2 | 11.9 | 11.6 | 17.2 | 5.6 | 5.3 | 6.1 |

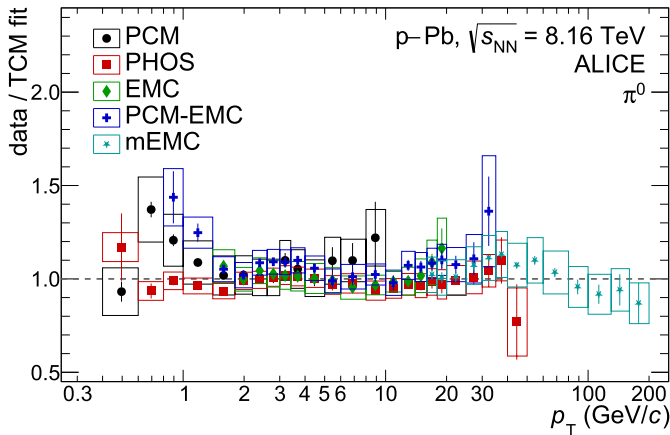


Fig. 2. Ratio of the neutral pion invariant differential cross sections to the two-component model (TCM) fit of the combined spectrum for the different reconstruction techniques PCM, PCM-EMC, EMC, PHOS and mEMC in p-Pb collisions at $\sqrt{s_{\text{NN}}} = 8.16$ TeV. Statistical uncertainties are given by the vertical error bars while systematic uncertainties are shown as boxes.

sections are between 5(8)% and 20(27)% and, due to uncertainty cancellations and correlations, between 7% and 24% on the η/π^0 ratio. For the $R_{p\text{Pb}}$, the p_T -independent uncertainties cancel as well as a fraction of the remaining uncertainties resulting in a total uncertainty between 4(11)% and 25(32)%. A tabulated overview of the systematic uncertainty contributions for selected p_T -intervals is given in Table 2.

5. Results

The invariant differential cross sections and $R_{p\text{Pb}}$ measured by each method are consistent within their uncertainties, as shown in Fig. 2. For the calculation of $R_{p\text{Pb}}$ the spectra are shifted in the y -direction, while for the cross sections they are shifted

along the p_T -axis to account for the finite bin width [46]. They were combined using the Best Linear Unbiased Estimate (BLUE) method [39,40] accounting for the partially correlated uncertainties. The resulting π^0 and η invariant differential cross sections for p-Pb collisions at $\sqrt{s_{\text{NN}}} = 8.16$ TeV are shown in Fig. 3 together with the π^0 cross section in pp collisions at $\sqrt{s} = 8$ TeV. In both cases, the high p_T reach of $p_T = 200$ GeV/c for the π^0 meson was enabled by the mEMC method, which allowed to significantly extend the previous pp measurement beyond 35 GeV/c [27]. The data is compared to a two-component model (TCM) fit [47], NLO calculations [41–43], and PYTHIA 8 [33,44] predictions using different nPDFs [9,10,45]. NLO calculations using the CT18 [48] PDF or nCTEQ15 [9] nPDF together with DSS14 [41] or AESSS [42] fragmentation functions generally overestimate the π^0 and η spectra, while predicting a steeper falling spectrum at high p_T . Additional NLO calculations based on the more recent NNFF1.0 [43] fragmentation functions are generally in good agreement with the data but tend to underestimate the spectra at low p_T . In Fig. 3 they are shown with factorization and renormalization scales varied from $\mu = p_T$ to $\mu = 0.5p_T$ and $2p_T$ and indicated by bands. PYTHIA 8 [33] calculations using EPPS16 [10] and nCTEQ15 [9] nPDFs describe the data, however without fully capturing the shape of the π^0 spectra, in particular at low and intermediate p_T , and with a tendency to underestimate the η spectra. For the η/π^0 ratio, presented in Fig. 3f, the differences in the shape and scale between data and calculations approximately cancel. The ratio is rather well described by the predictions and is consistent over the full p_T range between both collision systems. For $p_T > 4$ GeV/c, the η/π^0 ratio is $C_{p\text{Pb}}^{\eta/\pi^0} = 0.479 \pm 0.009(\text{stat}) \pm 0.010(\text{syst})$, consistent with the previous measurement at a lower center-of-mass energy [6] and with $C_{pp}^{\eta/\pi^0} = 0.473 \pm 0.006(\text{stat}) \pm 0.011(\text{syst})$, the reevaluated η/π^0 ratio in pp collisions at 8 TeV.

To provide the pp reference for the $R_{p\text{Pb}}$, the pp spectra measured at $\sqrt{s} = 8$ TeV were scaled to the p-Pb collision energy and

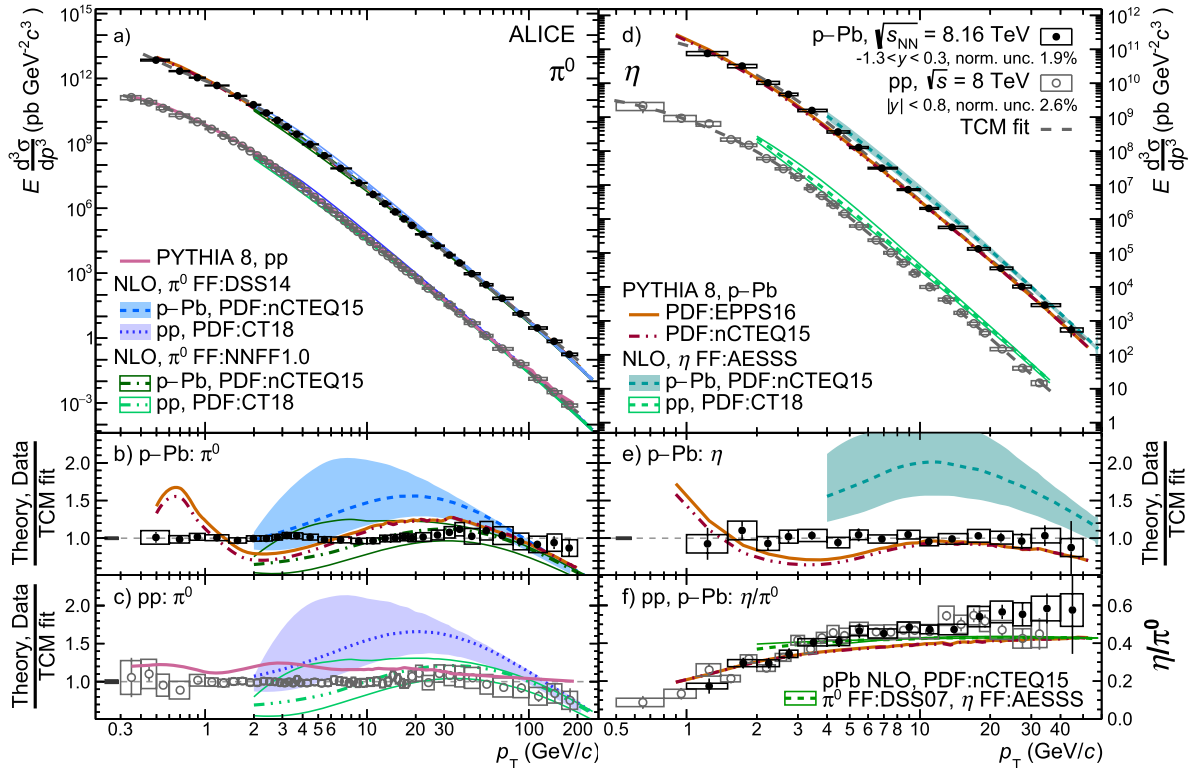


Fig. 3. Neutral pion a) and η meson d) cross sections for pp collisions at $\sqrt{s} = 8$ TeV and p-Pb collisions at $\sqrt{s_{NN}} = 8.16$ TeV together with TCM fits, NLO calculations [41–43] and PYTHIA 8 [33,44] predictions using different (n)PDFs [9,10,45]. Statistical uncertainties are shown as vertical bars; the systematic uncertainties as boxes. The ratios of the π^0 spectra in p-Pb and pp collisions to the TCM fits are shown in panel b) and c), respectively, together with the ratios of the calculations to the fits; panel e) shows the same for η mesons in p-Pb collisions. In panel f) the η/π^0 ratios in pp and p-Pb collisions are compared to theory predictions. The normalization uncertainty in the spectra ratio panels is indicated as a solid gray box around unity.

corrected for the rapidity difference, using the ratio of π^0 spectra generated with PYTHIA 8 Monash 2013 [44] for both kinematic regions, leading to a 1–2% increase over the whole p_T range. The resulting R_{pPb} at $\sqrt{s_{NN}} = 8.16$ TeV is shown in Fig. 4a for both mesons together with theory predictions and in Fig. 4b compared to data taken at $\sqrt{s_{NN}} = 5.02$ TeV. In the intermediate p_T region, the charged particle R_{pPb} exhibits an enhancement compared to the π^0 data, which is historically attributed to the stronger Cronin effect for baryons [49,50]. For $p_T > 10$ GeV/c, no deviation from unity is observed within uncertainties for both mesons, consistent with predictions and the ALICE π^0 and h^\pm measurements at $\sqrt{s_{NN}} = 5.02$ TeV [6,51], in contrast to the moderate enhancement for charged hadrons seen by the CMS experiment [5]. Fitting with a constant function resulted in 1.00 ± 0.01 (0.96 ± 0.04) with a χ^2/NDF of 1.04 (0.45) for the π^0 (η) meson. Based on the spectral slopes, the data disfavor a more than 1% relative energy loss or an induced constant p_T -shift of more than 100 MeV from final-state effects in the region between 10 and 20 GeV/c for both mesons, consistent with the calculations in Ref. [18].

For $p_T < 10$ GeV/c, a suppression of similar magnitude is observed for both mesons within uncertainties. The suppression is described by NLO calculations using EPPS16 [10] and nCTEQ15 [9] nPDFs (the latter tends to underpredict the data below 5 GeV/c), as well as by models using gluon recombination as the CGC-based calculations [12] or parton energy loss in cold nuclear matter in the framework of fully coherent energy loss (FCEL) [13].

The comparison of the π^0 R_{pPb} to the previous measurement at $\sqrt{s_{NN}} = 5.02$ TeV [6], as shown in Fig. 4c, is consistent with unity within uncertainties, but the data hints at a stronger suppression with increasing center-of-mass energy. A stronger suppression could originate from larger shadowing in the nPDFs, which due to the smaller x probed at 8.16 TeV predict a ratio of about 0.98

in the low p_T region, or from the increasing relevance of gluon saturation, as indicated by the CGC calculation [12]. The FCEL calculation predicts a negligible difference between the two collision energies excluding coherent energy loss as the cause of a stronger suppression. A constant fit for $p_T < 10$ GeV/c yields a ratio of $0.93 \pm 0.02_{\text{tot}} \pm 0.06_{\text{norm}}$, where the normalization uncertainty is dominated by the interpolation of the π^0 reference spectrum at 5.02 TeV.

6. Conclusion

In summary, cross sections for π^0 and η mesons in p-Pb collisions at $\sqrt{s_{NN}} = 8.16$ TeV were measured for $0.4 < p_T < 200$ GeV/c and $1.0 < p_T < 50$ GeV/c, respectively, providing constraints for nuclear parton distributions and fragmentation functions over an unprecedented kinematic range for light mesons. By extending the reference π^0 measurement in pp collisions at $\sqrt{s} = 8$ TeV to the same p_T range using the mEMC method, the R_{pPb} for π^0 was measured up to 200 GeV/c. The R_{pPb} is consistent with unity above 10 GeV/c, as expected from calculations without parton energy loss, and strongly suppressed at low p_T , consistent with theory predictions that also include gluon shadowing or saturation effects.

Declaration of competing interest

The authors declare that they have no known competing financial interests or personal relationships that could have appeared to influence the work reported in this paper.

Acknowledgements

We thank Werner Vogelsang for providing the pQCD calculations.

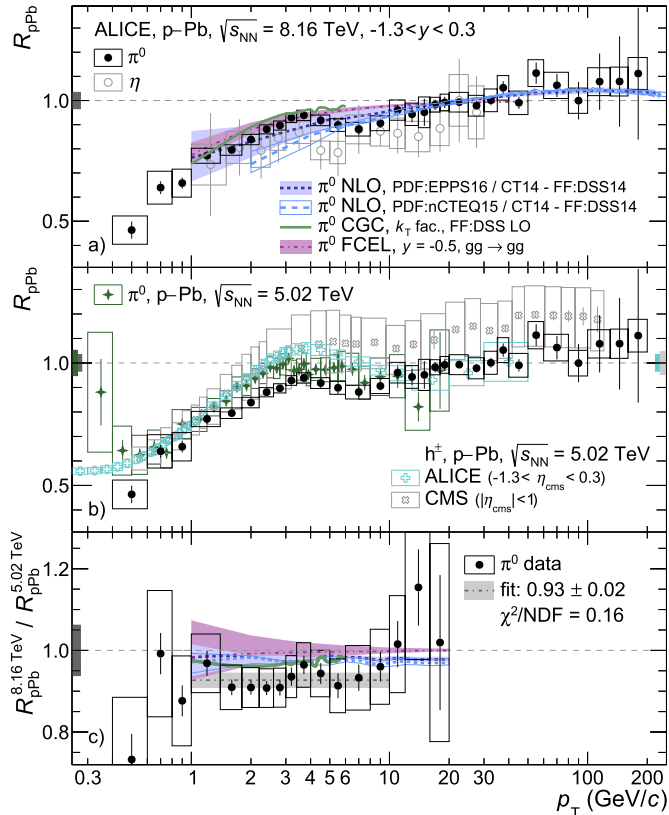


Fig. 4. a) R_{pPb} for π^0 and η mesons in p-Pb collisions at $\sqrt{s_{NN}} = 8.16$ TeV together with NLO [9,10], CGC [12] and FCEL [13] predictions. b) R_{pPb} for π^0 at $\sqrt{s_{NN}} = 8.16$ TeV compared with π^0 [6] and charged hadron measurements [5,51] at $\sqrt{s_{NN}} = 5.02$ TeV. c) Ratio of the π^0 R_{pPb} at $\sqrt{s_{NN}} = 8.16$ TeV to that at $\sqrt{s_{NN}} = 5.02$ TeV together with corresponding CGC and FCEL model predictions. Statistical uncertainties are shown as vertical bars; the systematic uncertainties as boxes. The overall normalization uncertainties are indicated as solid boxes around unity and amount to 3.4% in a) and b), and to 6.2% in c).

The ALICE Collaboration would like to thank all its engineers and technicians for their invaluable contributions to the construction of the experiment and the CERN accelerator teams for the outstanding performance of the LHC complex. The ALICE Collaboration gratefully acknowledges the resources and support provided by all Grid centers and the Worldwide LHC Computing Grid (WLCG) collaboration. The ALICE Collaboration acknowledges the following funding agencies for their support in building and running the ALICE detector: A.I. Alikhanyan National Science Laboratory (Yerevan Physics Institute) Foundation (ANSL), State Committee of Science and World Federation of Scientists (WFS), Armenia; Austrian Academy of Sciences, Austrian Science Fund (FWF): [M 2467-N36] and Nationalstiftung für Forschung, Technologie und Entwicklung, Austria; Ministry of Communications and High Technologies, National Nuclear Research Center, Azerbaijan; Conselho Nacional de Desenvolvimento Científico e Tecnológico (CNPq), Financiadora de Estudos e Projetos (Finep), Fundação de Amparo à Pesquisa do Estado de São Paulo (FAPESP) and Universidade Federal do Rio Grande do Sul (UFRGS), Brazil; Ministry of Education of China (MOEC), Ministry of Science & Technology of China (MSTC) and National Natural Science Foundation of China (NSFC), China; Ministry of Science and Education and Croatian Science Foundation, Croatia; Centro de Aplicaciones Tecnológicas y Desarrollo Nuclear (CEADEN), Cubaenergía, Cuba; Ministry of Education, Youth and Sports of the Czech Republic, Czech Republic; The Danish Council for Independent Research | Natural Sciences, the Villum Fonden and Danish National Research Foundation (DNRF), Denmark; Helsinki Institute of Physics (HIP), Finland; Commissariat à

l'Énergie Atomique (CEA) and Institut National de Physique Nucléaire et de Physique des Particules (IN2P3) and Centre National de la Recherche Scientifique (CNRS), France; Bundesministerium für Bildung und Forschung (BMBF) and GSI Helmholtzzentrum für Schwerionenforschung GmbH, Germany; General Secretariat for Research and Technology, Ministry of Education, Research and Religions, Greece; National Research, Development and Innovation Office, Hungary; Department of Atomic Energy, Government of India (DAE), Department of Science and Technology, Government of India (DST), University Grants Commission, Government of India (UGC) and Council of Scientific and Industrial Research (CSIR), India; Indonesian Institute of Science, Indonesia; Istituto Nazionale di Fisica Nucleare (INFN), Italy; Institute for Innovative Science and Technology, Nagasaki Institute of Applied Science (IIST), Japanese Ministry of Education, Culture, Sports, Science and Technology (MEXT) and Japan Society for the Promotion of Science (JSPS) KAKENHI, Japan; Consejo Nacional de Ciencia (CONACYT) y Tecnología, through Fondo de Cooperación Internacional en Ciencia y Tecnología (FONCICYT) and Dirección General de Asuntos del Personal Académico (DGAPA), Mexico; Nederlandse Organisatie voor Wetenschappelijk Onderzoek (NWO), Netherlands; The Research Council of Norway, Norway; Commission on Science and Technology for Sustainable Development in the South (COMSATS), Pakistan; Pontificia Universidad Católica del Perú, Peru; Ministry of Education and Science, National Science Centre and WUT ID-UB, Poland; Korea Institute of Science and Technology Information and National Research Foundation and Scientific Research, Institute of Atomic Physics and Ministry of Research and Innovation and Institute of Atomic Physics, Romania; Joint Institute for Nuclear Research (JINR), Ministry of Education and Science of the Russian Federation, National Research Centre Kurchatov Institute, Russian Science Foundation and Russian Foundation for Basic Research, Russia; Ministry of Education, Science, Research and Sport of the Slovak Republic, Slovakia; National Research Foundation of South Africa, South Africa; Swedish Research Council (VR) and Knut and Alice Wallenberg Foundation (KAW), Sweden; European Organization for Nuclear Research, Switzerland; Suranaree University of Technology (SUT), National Science and Technology Development Agency (NSDTA) and Office of the Higher Education Commission under NRU project of Thailand, Thailand; Turkish Atomic Energy Agency (TAEK), Turkey; National Academy of Sciences of Ukraine, Ukraine; Science and Technology Facilities Council (STFC), United Kingdom; National Science Foundation of the United States of America (NSF) and United States Department of Energy, Office of Nuclear Physics (DOE NP), United States of America.

References

- [1] N. Brambilla, et al., QCD and strongly coupled gauge theories: challenges and perspectives, *Eur. Phys. J. C* 74 (10) (2014) 2981, arXiv:1404.3723 [hep-ph].
- [2] C. Salgado, et al., Proton-nucleus collisions at the LHC: scientific opportunities and requirements, *J. Phys. G* 39 (2012) 015010, arXiv:1105.3919 [hep-ph].
- [3] ALICE Collaboration, B. Abelev, et al., Transverse momentum dependence of inclusive primary charged-particle production in p-Pb collisions at $\sqrt{s_{NN}} = 5.02$ TeV, *Eur. Phys. J. C* 74 (9) (2014) 3054, arXiv:1405.2737 [nucl-ex].
- [4] ATLAS Collaboration, G. Aad, et al., Transverse momentum, rapidity, and centrality dependence of inclusive charged-particle production in $\sqrt{s_{NN}} = 5.02$ TeV p-Pb collisions measured by the ATLAS experiment, *Phys. Lett. B* 763 (2016) 313–336, arXiv:1605.06436 [hep-ex].
- [5] CMS Collaboration, V. Khachatryan, et al., Charged-particle nuclear modification factors in Pb-Pb and p-Pb collisions at $\sqrt{s_{NN}} = 5.02$ TeV, *J. High Energy Phys.* 04 (2017) 039, arXiv:1611.01664 [nucl-ex].
- [6] ALICE Collaboration, S. Acharya, et al., Neutral pion and η meson production in p-Pb collisions at $\sqrt{s_{NN}} = 5.02$ TeV, *Eur. Phys. J. C* 78 (8) (2018) 624, arXiv:1801.07051 [nucl-ex].
- [7] PHENIX Collaboration, S. Adler, et al., Absence of suppression in particle production at large transverse momentum in $\sqrt{s_{NN}} = 200$ GeV d-Au collisions, *Phys. Rev. Lett.* 91 (2003) 072303, arXiv:nucl-ex/0306021.

- [8] STAR Collaboration, J. Adams, et al., Evidence from d–Au measurements for final state suppression of high p_T hadrons in Au–Au collisions at RHIC, *Phys. Rev. Lett.* 91 (2003) 072304, arXiv:nucl-ex/0306024.
- [9] K. Kovarik, et al., nCTEQ15 - global analysis of nuclear parton distributions with uncertainties in the CTEQ framework, *Phys. Rev. D* 93 (8) (2016) 085037, arXiv:1509.00792 [hep-ph].
- [10] K.J. Eskola, P. Paakkinen, H. Paukkunen, C.A. Salgado, EPPS16: nuclear parton distributions with LHC data, *Eur. Phys. J. C* 77 (3) (2017) 163, arXiv:1612.05741 [hep-ph].
- [11] F. Gelis, E. Iancu, J. Jalilian-Marian, R. Venugopalan, The color glass condensate, *Annu. Rev. Nucl. Part. Sci.* 60 (2010) 463–489, arXiv:1002.0333 [hep-ph].
- [12] T. Lappi, H. Mäntysaari, Single inclusive particle production at high energy from HERA data to proton–nucleus collisions, *Phys. Rev. D* 88 (2013) 114020, arXiv:1309.6963 [hep-ph].
- [13] F. Arleo, F. Cougoulic, S. Peigné, Fully coherent energy loss effects on light hadron production in pA collisions, *J. High Energy Phys.* 09 (2020) 190, arXiv:2003.06337 [hep-ph].
- [14] ALICE Collaboration, B.B. Abelev, et al., Multiparticle azimuthal correlations in p-Pb and Pb-Pb collisions at the CERN Large Hadron Collider, *Phys. Rev. C* 90 (5) (2014) 054901, arXiv:1406.2474 [nucl-ex].
- [15] CMS Collaboration, V. Khachatryan, et al., Evidence for collective multiparticle correlations in p-Pb collisions, *Phys. Rev. Lett.* 115 (1) (2015) 012301, arXiv:1502.05382 [nucl-ex].
- [16] CMS Collaboration, A.M. Sirunyan, et al., Observation of correlated azimuthal anisotropy Fourier harmonics in pp and $p + Pb$ collisions at the LHC, *Phys. Rev. Lett.* 120 (9) (2018) 092301, arXiv:1709.09189 [nucl-ex].
- [17] I. Vitev, Non-Abelian energy loss in cold nuclear matter, *Phys. Rev. C* 75 (2007) 064906, arXiv:hep-ph/0703002.
- [18] A. Huss, A. Kurkela, A. Mazeliauskas, R. Paatelainen, W. van der Schee, U.A. Wiedemann, Predicting parton energy loss in small collision systems, arXiv:2007.13758 [hep-ph].
- [19] ALICE Collaboration, K. Aamodt, et al., The ALICE experiment at the CERN LHC, *J. Instrum.* 3 (2008) S08002.
- [20] ALICE Collaboration, B. Abelev, et al., Performance of the ALICE experiment at the CERN LHC, *Int. J. Mod. Phys. A* 29 (2014) 1430044, arXiv:1402.4476 [nucl-ex].
- [21] ALICE Collaboration, K. Aamodt, et al., Alignment of the ALICE Inner Tracking System with cosmic-ray tracks, *J. Instrum.* 5 (2010) P03003, arXiv:1001.0502 [physics.ins-det].
- [22] ALICE EMCal Collaboration, U. Abeyssekara, et al., ALICE EMCal physics performance report, arXiv:1008.0413 [physics.ins-det].
- [23] J. Allen, et al., ALICE DCal: an addendum to the EMCal technical design report di-jet and hadron-jet correlation measurements in ALICE, CERN-LHCC-2010-011. ALICE-TDR-14-add-1, <http://cds.cern.ch/record/1272952>.
- [24] ALICE Collaboration, G. Dellacasa, et al., ALICE technical design report of the photon spectrometer (PHOS), CERN-LHCC-99-04, <http://cds.cern.ch/record/381432>.
- [25] ALICE Collaboration, E. Abbas, et al., Performance of the ALICE VZERO system, *J. Instrum.* 8 (2013) P10016, arXiv:1306.3130 [nucl-ex].
- [26] ALICE Collaboration, S. Acharya, et al., ALICE luminosity determination for p-Pb collisions at $\sqrt{s_{NN}} = 8.16$ TeV, ALICE-PUBLIC-2018-002, <https://cds.cern.ch/record/2314660>.
- [27] ALICE Collaboration, S. Acharya, et al., π^0 and η meson production in proton–proton collisions at $\sqrt{s} = 8$ TeV, *Eur. Phys. J. C* 78 (3) (2018) 263, arXiv:1708.08745 [hep-ex].
- [28] ALICE Collaboration, C.W. Fabjan, et al., ALICE: physics performance report, volume II, *J. Phys. G* 32 (2006) 1295–2040.
- [29] ALICE Collaboration, S. Acharya, et al., Measurement of the inclusive isolated photon production cross section in pp collisions at $\sqrt{s} = 7$ TeV, *Eur. Phys. J. C* 79 (11) (2019) 896, arXiv:1906.01371 [nucl-ex].
- [30] ALICE Collaboration, S. Acharya, et al., Calibration of the photon spectrometer PHOS of the ALICE experiment, *J. Instrum.* 14 (05) (2019) P05025, arXiv:1902.06145 [physics.ins-det].
- [31] ALICE Collaboration, S. Acharya, et al., Production of π^0 and η mesons up to high transverse momentum in pp collisions at 2.76 TeV, *Eur. Phys. J. C* 77 (5) (2017) 339, arXiv:1702.00917 [hep-ex].
- [32] ALICE Collaboration, S. Acharya, et al., Supplemental material for “Nuclear modification factor of light neutral mesons up to high transverse momentum in p–Pb collisions at $\sqrt{s_{NN}} = 8.16$ TeV”, CERN-EP-2021-053, <https://cds.cern.ch/record/2759761>, Aug. 2021.
- [33] T. Sjostrand, S. Mrenna, P.Z. Skands, A brief introduction to PYTHIA 8.1, *Comput. Phys. Commun.* 178 (2008) 852–867, arXiv:0710.3820 [hep-ph].
- [34] S. Alioli, P. Nason, C. Oleari, E. Re, A general framework for implementing NLO calculations in shower Monte Carlo programs: the POWHEG BOX, *J. High Energy Phys.* 06 (2010) 043, arXiv:1002.2581 [hep-ph].
- [35] S. Alioli, P. Nason, C. Oleari, E. Re, NLO vector-boson production matched with shower in POWHEG, *J. High Energy Phys.* 07 (2008) 060, arXiv:0805.4802 [hep-ph].
- [36] R. Brun, F. Bruyant, F. Carminati, S. Giani, M. Maire, A. McPherson, G. Patrick, L. Urban, GEANT: detector description and simulation tool, CERN-W5013, <https://cds.cern.ch/record/1082634>.
- [37] S. Roesler, R. Engel, J. Ranft, The Monte Carlo event generator DPMJET-III, in: International Conference on Advanced Monte Carlo for Radiation Physics, Particle Transport Simulation and Applications (MC 2000), 2000, pp. 1033–1038, arXiv:hep-ph/0012252.
- [38] ALICE Collaboration, S. Acharya, et al., Direct photon production at low transverse momentum in proton–proton collisions at $\sqrt{s} = 2.76$ and 8 TeV, *Phys. Rev. C* 99 (2) (2019) 024912, arXiv:1803.09857 [nucl-ex].
- [39] A. Valassi, R. Chierici, Information and treatment of unknown correlations in the combination of measurements using the BLUE method, *Eur. Phys. J. C* 74 (2014) 2717, arXiv:1307.4003 [physics.data-an].
- [40] L. Lyons, D. Gibaut, P. Clifford, How to combine correlated estimates of a single physical quantity, *Nucl. Instrum. Methods Phys. Res., Sect. A* 270 (1988) 110.
- [41] D. de Florian, R. Sassot, M. Epele, R.J. Hernández-Pinto, M. Stratmann, Parton-to-pion fragmentation reloaded, *Phys. Rev. D* 91 (1) (2015) 014035, arXiv:1410.6027 [hep-ph].
- [42] C.A. Aidala, F. Ellinghaus, R. Sassot, J.P. Seele, M. Stratmann, Global analysis of fragmentation functions for η mesons, *Phys. Rev. D* 83 (2011) 034002, arXiv:1009.6145 [hep-ph].
- [43] NNPDF Collaboration, V. Bertone, S. Carrazza, N.P. Hartland, E.R. Nocera, J. Rojo, A determination of the fragmentation functions of pions, kaons, and protons with faithful uncertainties, *Eur. Phys. J. C* 77 (8) (2017) 516, arXiv:1706.07049 [hep-ph].
- [44] P. Skands, S. Carrazza, J. Rojo, Tuning PYTHIA 8.1: the Monash 2013 tune, *Eur. Phys. J. C* 74 (8) (2014) 3024, arXiv:1404.5630 [hep-ph].
- [45] T.-J. Hou, et al., New CTEQ global analysis of quantum chromodynamics with high-precision data from the LHC, *Phys. Rev. D* 103 (1) (2021) 014013, arXiv:1912.10053 [hep-ph].
- [46] G. Lafferty, T. Wyatt, Where to stick your data points: the treatment of measurements within wide bins, *Nucl. Instrum. Methods Phys. Res., Sect. A* 355 (1995) 541–547.
- [47] A. Bylinkin, N.S. Chernyavskaya, A.A. Rostovtsev, Predictions on the transverse momentum spectra for charged particle production at LHC-energies from a two component model, *Eur. Phys. J. C* 75 (4) (2015) 166, arXiv:1501.05235 [hep-ph].
- [48] M. Guzzi, P. Nadolsky, E. Berger, H.-L. Lai, F. Olness, C.P. Yuan, CT10 parton distributions and other developments in the global QCD analysis, arXiv:1101.0561 [hep-ph].
- [49] J.W. Cronin, H.J. Frisch, M.J. Shochet, J.P. Boymond, R. Mermod, P.A. Piroue, R.L. Sumner, Production of hadrons with large transverse momentum at 200, 300, and 400 GeV, *Phys. Rev. D* 11 (1975) 3105–3123.
- [50] A.H. Rezaeian, Z. Lu, Cronin effect for protons and pions in high-energy pA collisions, *Nucl. Phys. A* 826 (2009) 198–210, arXiv:0810.4942 [hep-ph].
- [51] ALICE Collaboration, S. Acharya, et al., Transverse momentum spectra and nuclear modification factors of charged particles in pp, p–Pb and Pb–Pb collisions at the LHC, *J. High Energy Phys.* 11 (2018) 013, arXiv:1802.09145 [nucl-ex].

ALICE Collaboration

S. Acharya¹⁴², D. Adamová⁹⁷, A. Adler⁷⁵, J. Adolfsson⁸², G. Aglieri Rinella³⁵, M. Agnello³¹, N. Agrawal⁵⁵, Z. Ahammed¹⁴², S. Ahmad¹⁶, S.U. Ahn⁷⁷, I. Ahuja³⁹, Z. Akbar⁵², A. Akindinov⁹⁴, M. Al-Turany¹⁰⁹, S.N. Alam⁴¹, D. Aleksandrov⁹⁰, B. Alessandro⁶⁰, H.M. Alfanda⁷, R. Alfaro Molina⁷², B. Ali¹⁶, Y. Ali¹⁴, A. Alici²⁶, N. Alizadehvandchali¹²⁶, A. Alkin³⁵, J. Alme²¹, T. Alt⁶⁹, L. Altenkamper²¹, I. Altsybeev¹¹⁴, M.N. Anaam⁷, C. Andrei⁴⁹, D. Andreou⁹², A. Andronic¹⁴⁵, M. Angeletti³⁵, V. Anguelov¹⁰⁶, F. Antinori⁵⁸, P. Antonioli⁵⁵, C. Anuj¹⁶, N. Apadula⁸¹, L. Aphecetche¹¹⁶, H. Appelshäuser⁶⁹, S. Arcelli²⁶, R. Arnaldi⁶⁰, I.C. Arsene²⁰, M. Arslandok^{147,106}, A. Augustinus³⁵, R. Averbek¹⁰⁹, S. Aziz⁷⁹, M.D. Azmi¹⁶, A. Badalà⁵⁷, Y.W. Baek⁴², X. Bai¹⁰⁹, R. Bailhache⁶⁹, Y. Bailung⁵¹,

R. Bala¹⁰³, A. Balbino³¹, A. Baldisseri¹³⁹, M. Ball⁴⁴, D. Banerjee⁴, R. Barbera²⁷, L. Barioglio^{107,25}, M. Barlou⁸⁶, G.G. Barnaföldi¹⁴⁶, L.S. Barnby⁹⁶, V. Barret¹³⁶, C. Bartels¹²⁹, K. Barth³⁵, E. Bartsch⁶⁹, F. Baruffaldi²⁸, N. Bastid¹³⁶, S. Basu⁸², G. Batigne¹¹⁶, B. Batyunya⁷⁶, D. Bauri⁵⁰, J.L. Bazo Alba¹¹³, I.G. Bearden⁹¹, C. Beattie¹⁴⁷, I. Belikov¹³⁸, A.D.C. Bell Hechavarria¹⁴⁵, F. Bellini^{26,35}, R. Bellwied¹²⁶, S. Belokurova¹¹⁴, V. Belyaev⁹⁵, G. Bencedi⁷⁰, S. Beole²⁵, A. Bercuci⁴⁹, Y. Berdnikov¹⁰⁰, A. Berdnikova¹⁰⁶, D. Berenyi¹⁴⁶, L. Bergmann¹⁰⁶, M.G. Besoiu⁶⁸, L. Betev³⁵, P.P. Bhaduri¹⁴², A. Bhasin¹⁰³, I.R. Bhat¹⁰³, M.A. Bhat⁴, B. Bhattacharjee⁴³, P. Bhattacharya²³, L. Bianchi²⁵, N. Bianchi⁵³, J. Bielčik³⁸, J. Bielčíková⁹⁷, J. Biernat¹¹⁹, A. Bilandzic¹⁰⁷, G. Biro¹⁴⁶, S. Biswas⁴, J.T. Blair¹²⁰, D. Blau⁹⁰, M.B. Blidaru¹⁰⁹, C. Blume⁶⁹, G. Boca²⁹, F. Bock⁹⁸, A. Bogdanov⁹⁵, S. Boi²³, J. Bok⁶², L. Boldizsár¹⁴⁶, A. Bolozdynya⁹⁵, M. Bombara³⁹, P.M. Bond³⁵, G. Bonomi¹⁴¹, H. Borel¹³⁹, A. Borissov⁸³, H. Bossi¹⁴⁷, E. Botta²⁵, L. Bratrud⁶⁹, P. Braun-Munzinger¹⁰⁹, M. Bregant¹²², M. Broz³⁸, G.E. Bruno^{108,34}, M.D. Buckland¹²⁹, D. Budnikov¹¹⁰, H. Buesching⁶⁹, S. Bufalino³¹, O. Bugnon¹¹⁶, P. Buhler¹¹⁵, Z. Buthelezi^{73,133}, J.B. Butt¹⁴, S.A. Bysiak¹¹⁹, D. Caffarri⁹², M. Cai^{28,7}, H. Caines¹⁴⁷, A. Caliva¹⁰⁹, E. Calvo Villar¹¹³, J.M.M. Camacho¹²¹, R.S. Camacho⁴⁶, P. Camerini²⁴, F.D.M. Canedo¹²², A.A. Capon¹¹⁵, F. Carnesecchi^{35,26}, R. Caron¹³⁹, J. Castillo Castellanos¹³⁹, E.A.R. Casula²³, F. Catalano³¹, C. Ceballos Sanchez⁷⁶, P. Chakraborty⁵⁰, S. Chandra¹⁴², S. Chapeland³⁵, M. Chartier¹²⁹, S. Chattopadhyay¹⁴², S. Chattopadhyay¹¹¹, A. Chauvin²³, T.G. Chavez⁴⁶, C. Cheshkov¹³⁷, B. Cheynis¹³⁷, V. Chibante Barroso³⁵, D.D. Chinellato¹²³, S. Cho⁶², P. Chochula³⁵, P. Christakoglou⁹², C.H. Christensen⁹¹, P. Christiansen⁸², T. Chujo¹³⁵, C. Cicalo⁵⁶, L. Cifarelli²⁶, F. Cindolo⁵⁵, M.R. Ciupek¹⁰⁹, G. Clai^{55,II}, J. Cleymans^{125,I}, F. Colamaria⁵⁴, J.S. Colburn¹¹², D. Colella^{108,54,34,146}, A. Collu⁸¹, M. Colocci^{35,26}, M. Concas^{60,III}, G. Conesa Balbastre⁸⁰, Z. Conesa del Valle⁷⁹, G. Contin²⁴, J.G. Contreras³⁸, T.M. Cormier⁹⁸, P. Cortese³², M.R. Cosentino¹²⁴, F. Costa³⁵, S. Costanza²⁹, P. Crochet¹³⁶, E. Cuautele⁷⁰, P. Cui⁷, L. Cunqueiro⁹⁸, A. Dainese⁵⁸, F.P.A. Damas^{116,139}, M.C. Danisch¹⁰⁶, A. Danu⁶⁸, I. Das¹¹¹, P. Das⁸⁸, P. Das⁴, S. Das⁴, S. Dash⁵⁰, S. De⁸⁸, A. De Caro³⁰, G. de Cataldo⁵⁴, L. De Cilladi²⁵, J. de Cuveland⁴⁰, A. De Falco²³, D. De Gruttola³⁰, N. De Marco⁶⁰, C. De Martin²⁴, S. De Pasquale³⁰, S. Deb⁵¹, H.F. Degenhardt¹²², K.R. Deja¹⁴³, L. Dello Stritto³⁰, S. Delsanto²⁵, W. Deng⁷, P. Dhankher¹⁹, D. Di Bari³⁴, A. Di Mauro³⁵, R.A. Diaz⁸, T. Dietel¹²⁵, Y. Ding^{137,7}, R. Divià³⁵, D.U. Dixit¹⁹, Ø. Djuvsland²¹, U. Dmitrieva⁶⁴, J. Do⁶², A. Dobrin⁶⁸, B. Dönigus⁶⁹, O. Dordic²⁰, A.K. Dubey¹⁴², A. Dubla^{109,92}, S. Dudi¹⁰², M. Dukhishyam⁸⁸, P. Dupieux¹³⁶, N. Dzalaiova¹³, T.M. Eder¹⁴⁵, R.J. Ehlers⁹⁸, V.N. Eikeland²¹, D. Elia⁵⁴, B. Erasmus¹¹⁶, F. Ercolessi²⁶, F. Erhardt¹⁰¹, A. Erokhin¹¹⁴, M.R. Ersdal²¹, B. Espagnon⁷⁹, G. Eulisse³⁵, D. Evans¹¹², S. Evdokimov⁹³, L. Fabbietti¹⁰⁷, M. Faggin²⁸, J. Faivre⁸⁰, F. Fan⁷, A. Fantoni⁵³, M. Fasel⁹⁸, P. Fedichio³¹, A. Feliciello⁶⁰, G. Feofilov¹¹⁴, A. Fernández Téllez⁴⁶, A. Ferrero¹³⁹, A. Ferretti²⁵, V.J.G. Feuillard¹⁰⁶, J. Figiel¹¹⁹, S. Filchagin¹¹⁰, D. Finogeev⁶⁴, F.M. Fionda^{56,21}, G. Fiorenza^{35,108}, F. Flor¹²⁶, A.N. Flores¹²⁰, S. Foertsch⁷³, P. Foka¹⁰⁹, S. Fokin⁹⁰, E. Fragiaco⁶¹, E. Frajna¹⁴⁶, U. Fuchs³⁵, N. Funicello³⁰, C. Furget⁸⁰, A. Furs⁶⁴, J.J. Gaardhøje⁹¹, M. Gagliardi²⁵, A.M. Gago¹¹³, A. Gal¹³⁸, C.D. Galvan¹²¹, P. Ganoti⁸⁶, C. Garabatos¹⁰⁹, J.R.A. Garcia⁴⁶, E. Garcia-Solis¹⁰, K. Garg¹¹⁶, C. Gargiulo³⁵, A. Garibli⁸⁹, K. Garner¹⁴⁵, P. Gasik¹⁰⁹, E.F. Gauger¹²⁰, A. Gautam¹²⁸, M.B. Gay Ducati⁷¹, M. Germain¹¹⁶, J. Ghosh¹¹¹, P. Ghosh¹⁴², S.K. Ghosh⁴, M. Giacalone²⁶, P. Gianotti⁵³, P. Giubellino^{109,60}, P. Giubilato²⁸, A.M.C. Glaenger¹³⁹, P. Glässel¹⁰⁶, V. Gonzalez¹⁴⁴, L.H. González-Trueba⁷², S. Gorbunov⁴⁰, L. Görlich¹¹⁹, S. Gotovac³⁶, V. Grabski⁷², L.K. Graczykowski¹⁴³, L. Greiner⁸¹, A. Grelli⁶³, C. Grigoras³⁵, V. Grigoriev⁹⁵, A. Grigoryan^{1,I}, S. Grigoryan^{76,1}, O.S. Groettvik²¹, F. Grosa^{35,60}, J.F. Grosse-Oetringhaus³⁵, R. Grosso¹⁰⁹, G.G. Guardiano¹²³, R. Guernane⁸⁰, M. Guilbaud¹¹⁶, M. Guittiere¹¹⁶, K. Gulbrandsen⁹¹, T. Gunji¹³⁴, A. Gupta¹⁰³, R. Gupta¹⁰³, I.B. Guzman⁴⁶, S.P. Guzman⁴⁶, L. Gyulai¹⁴⁶, M.K. Habib¹⁰⁹, C. Hadjidakis⁷⁹, H. Hamagaki⁸⁴, G. Hamar¹⁴⁶, M. Hamid⁷, R. Hannigan¹²⁰, M.R. Haque^{143,88}, A. Harlanderova¹⁰⁹, J.W. Harris¹⁴⁷, A. Harton¹⁰, J.A. Hasenbichler³⁵, H. Hassan⁹⁸, D. Hatzifotiadou⁵⁵, P. Hauer⁴⁴, L.B. Havener¹⁴⁷, S. Hayashi¹³⁴, S.T. Heckel¹⁰⁷, E. Hellbär⁶⁹, H. Helstrup³⁷, T. Herman³⁸, E.G. Hernandez⁴⁶, G. Herrera Corral⁹, F. Herrmann¹⁴⁵, K.F. Hetland³⁷, H. Hillemanns³⁵, C. Hills¹²⁹, B. Hippolyte¹³⁸, B. Hofman⁶³, B. Hohlweger^{92,107}, J. Honermann¹⁴⁵, G.H. Hong¹⁴⁸, D. Horak³⁸, S. Hornung¹⁰⁹, R. Hosokawa¹⁵, P. Hristov³⁵, C. Huang⁷⁹, C. Hughes¹³², P. Huhn⁶⁹, T.J. Humanic⁹⁹, H. Hushnud¹¹¹, L.A. Husova¹⁴⁵, N. Hussain⁴³, D. Hutter⁴⁰, J.P. Iddon^{35,129}, R. Ilkaev¹¹⁰, H. Ilyas¹⁴, M. Inaba¹³⁵, G.M. Innocenti³⁵, M. Ippolitov⁹⁰, A. Isakov^{38,97}, M.S. Islam¹¹¹, M. Ivanov¹⁰⁹, V. Ivanov¹⁰⁰, V. Izucheev⁹³, B. Jacak⁸¹, N. Jacazio³⁵, P.M. Jacobs⁸¹, S. Jadlovská¹¹⁸, J. Jadlovsky¹¹⁸, S. Jaelani⁶³, C. Jahnke^{123,122}, M.J. Jakubowska¹⁴³, M.A. Janik¹⁴³, T. Janson⁷⁵, M. Jercic¹⁰¹, O. Jevons¹¹²,

F. Jonas^{98,145}, P.G. Jones¹¹², J.M. Jowett^{35,109}, J. Jung⁶⁹, M. Jung⁶⁹, A. Junique³⁵, A. Jusko¹¹², J. Kaewjai¹¹⁷, P. Kalinak⁶⁵, A. Kalweit³⁵, V. Kaplin⁹⁵, S. Kar⁷, A. Karasu Uysal⁷⁸, D. Karatovic¹⁰¹, O. Karavichev⁶⁴, T. Karavicheva⁶⁴, P. Karczmarczyk¹⁴³, E. Karpechev⁶⁴, A. Kazantsev⁹⁰, U. Kbschull⁷⁵, R. Keidel⁴⁸, D.L.D. Keijdener⁶³, M. Keil³⁵, B. Ketzer⁴⁴, Z. Khabanova⁹², A.M. Khan⁷, S. Khan¹⁶, A. Khanzadeev¹⁰⁰, Y. Kharlov⁹³, A. Khatun¹⁶, A. Khuntia¹¹⁹, B. Kileng³⁷, B. Kim^{17,62}, D. Kim¹⁴⁸, D.J. Kim¹²⁷, E.J. Kim⁷⁴, J. Kim¹⁴⁸, J.S. Kim⁴², J. Kim¹⁰⁶, J. Kim¹⁴⁸, J. Kim⁷⁴, M. Kim¹⁰⁶, S. Kim¹⁸, T. Kim¹⁴⁸, S. Kirsch⁶⁹, I. Kisel⁴⁰, S. Kiselev⁹⁴, A. Kisiel¹⁴³, J.L. Klay⁶, J. Klein³⁵, S. Klein⁸¹, C. Klein-Bösing¹⁴⁵, M. Kleiner⁶⁹, T. Klemenz¹⁰⁷, A. Kluge³⁵, A.G. Knospe¹²⁶, C. Kobdaj¹¹⁷, M.K. Köhler¹⁰⁶, T. Kollegger¹⁰⁹, A. Kondratyev⁷⁶, N. Kondratyeva⁹⁵, E. Kondratyuk⁹³, J. König⁶⁹, S.A. Königstorfer¹⁰⁷, P.J. Konopka^{35,2}, G. Kornakov¹⁴³, S.D. Koryciak², L. Koska¹¹⁸, A. Kotliarov⁹⁷, O. Kovalenko⁸⁷, V. Kovalenko¹¹⁴, M. Kowalski¹¹⁹, I. Králik⁶⁵, A. Kravčáková³⁹, L. Kreis¹⁰⁹, M. Krivda^{112,65}, F. Krizek⁹⁷, K. Krizkova Gajdosova³⁸, M. Kroesen¹⁰⁶, M. Krüger⁶⁹, E. Kryshen¹⁰⁰, M. Krzewicki⁴⁰, V. Kučera³⁵, C. Kuhn¹³⁸, P.G. Kuijer⁹², T. Kumaoka¹³⁵, D. Kumar¹⁴², L. Kumar¹⁰², N. Kumar¹⁰², S. Kundu^{35,88}, P. Kurashvili⁸⁷, A. Kurepin⁶⁴, A.B. Kurepin⁶⁴, A. Kuryakin¹¹⁰, S. Kuschpil⁹⁷, J. Kvapil¹¹², M.J. Kweon⁶², J.Y. Kwon⁶², Y. Kwon¹⁴⁸, S.L. La Pointe⁴⁰, P. La Rocca²⁷, Y.S. Lai⁸¹, A. Lakrathok¹¹⁷, M. Lamanna³⁵, R. Langoy¹³¹, K. Lapidus³⁵, P. Larionov⁵³, E. Laudi³⁵, L. Lautner^{35,107}, R. Lavicka³⁸, T. Lazareva¹¹⁴, R. Lea^{141,24}, J. Lee¹³⁵, J. Lehrbach⁴⁰, R.C. Lemmon⁹⁶, I. León Monzón¹²¹, E.D. Lesser¹⁹, M. Lettrich^{35,107}, P. Lévai¹⁴⁶, X. Li¹¹, X.L. Li⁷, J. Lien¹³¹, R. Lietava¹¹², B. Lim¹⁷, S.H. Lim¹⁷, V. Lindenstruth⁴⁰, A. Lindner⁴⁹, C. Lippmann¹⁰⁹, A. Liu¹⁹, J. Liu¹²⁹, I.M. Lofnes²¹, V. Loginov⁹⁵, C. Loizides⁹⁸, P. Loncar³⁶, J.A. Lopez¹⁰⁶, X. Lopez¹³⁶, E. López Torres⁸, J.R. Luhder¹⁴⁵, M. Lunardon²⁸, G. Luparello⁶¹, Y.G. Ma⁴¹, A. Maevskaya⁶⁴, M. Mager³⁵, T. Mahmoud⁴⁴, A. Maire¹³⁸, M. Malaev¹⁰⁰, Q.W. Malik²⁰, L. Malinina^{76,IV}, D. Mal'Kevich⁹⁴, N. Mallick⁵¹, P. Malzacher¹⁰⁹, G. Mandaglio^{33,57}, V. Manko⁹⁰, F. Manso¹³⁶, V. Manzari⁵⁴, Y. Mao⁷, J. Mareš⁶⁷, G.V. Margagliotti²⁴, A. Margotti⁵⁵, A. Marín¹⁰⁹, C. Markert¹²⁰, M. Marquard⁶⁹, N.A. Martin¹⁰⁶, P. Martinengo³⁵, J.L. Martinez¹²⁶, M.I. Martínez⁴⁶, G. Martínez García¹¹⁶, S. Masciocchi¹⁰⁹, M. Masera²⁵, A. Masoni⁵⁶, L. Massacrier⁷⁹, A. Mastroserio^{140,54}, A.M. Mathis¹⁰⁷, O. Matonoha⁸², P.F.T. Matuoka¹²², A. Matyja¹¹⁹, C. Mayer¹¹⁹, A.L. Mazuecos³⁵, F. Mazzaschi²⁵, M. Mazzilli^{35,54}, M.A. Mazzoni⁵⁹, J.E. Mdhului¹³³, A.F. Mechler⁶⁹, F. Meddi²², Y. Melikyan⁶⁴, A. Menchaca-Rocha⁷², E. Meninno^{115,30}, A.S. Menon¹²⁶, M. Meres¹³, S. Mhlanga^{125,73}, Y. Miake¹³⁵, L. Micheletti²⁵, L.C. Migliorin¹³⁷, D.L. Mihaylov¹⁰⁷, K. Mikhaylov^{76,94}, A.N. Mishra¹⁴⁶, D. Miśkowiec¹⁰⁹, A. Modak⁴, A.P. Mohanty⁶³, B. Mohanty⁸⁸, M. Mohisin Khan¹⁶, Z. Moravcova⁹¹, C. Mordasini¹⁰⁷, D.A. Moreira De Godoy¹⁴⁵, L.A.P. Moreno⁴⁶, I. Morozov⁶⁴, A. Morsch³⁵, T. Mrnjavac³⁵, V. Muccifora⁵³, E. Mudnic³⁶, D. Mühlheim¹⁴⁵, S. Muhuri¹⁴², J.D. Mulligan⁸¹, A. Mulliri²³, M.G. Munhoz¹²², R.H. Munzer⁶⁹, H. Murakami¹³⁴, S. Murray¹²⁵, L. Musa³⁵, J. Musinsky⁶⁵, C.J. Myers¹²⁶, J.W. Myrcha¹⁴³, B. Naik⁵⁰, R. Nair⁸⁷, B.K. Nandi⁵⁰, R. Nania⁵⁵, E. Nappi⁵⁴, M.U. Naru¹⁴, A.F. Nassirpour⁸², A. Nath¹⁰⁶, C. Nattrass¹³², A. Neagu²⁰, L. Nellen⁷⁰, S.V. Nesbo³⁷, G. Neskovic⁴⁰, D. Nesterov¹¹⁴, B.S. Nielsen⁹¹, S. Nikolaev⁹⁰, S. Nikulin⁹⁰, V. Nikulin¹⁰⁰, F. Noferini⁵⁵, S. Noh¹², P. Nomokonov⁷⁶, J. Norman¹²⁹, N. Novitzky¹³⁵, P. Nowakowski¹⁴³, A. Nyanin⁹⁰, J. Nystrand²¹, M. Ogino⁸⁴, A. Ohlson⁸², V.A. Okorokov⁹⁵, J. Oleniacz¹⁴³, A.C. Oliveira Da Silva¹³², M.H. Oliver¹⁴⁷, A. Onnerstad¹²⁷, C. Oppedisano⁶⁰, A. Ortiz Velasquez⁷⁰, T. Osako⁴⁷, A. Oskarsson⁸², J. Otwinowski¹¹⁹, K. Oyama⁸⁴, Y. Pachmayer¹⁰⁶, S. Padhan⁵⁰, D. Pagano¹⁴¹, G. Paic⁷⁰, A. Palasciano⁵⁴, J. Pan¹⁴⁴, S. Panebianco¹³⁹, P. Pareek¹⁴², J. Park⁶², J.E. Parkkila¹²⁷, S.P. Pathak¹²⁶, R.N. Patra^{103,35}, B. Paul²³, J. Pazzini¹⁴¹, H. Pei⁷, T. Peitzmann⁶³, X. Peng⁷, L.G. Pereira⁷¹, H. Pereira Da Costa¹³⁹, D. Peresunko⁹⁰, G.M. Perez⁸, S. Perrin¹³⁹, Y. Pestov⁵, V. Petráček³⁸, M. Petrovici⁴⁹, R.P. Pezzi⁷¹, S. Piano⁶¹, M. Pikna¹³, P. Pillot¹¹⁶, O. Pinazza^{55,35}, L. Pinsky¹²⁶, C. Pinto²⁷, S. Pisano⁵³, M. Płoskoń⁸¹, M. Planinic¹⁰¹, F. Pliquett⁶⁹, M.G. Poghosyan⁹⁸, B. Polichtchouk⁹³, S. Politano³¹, N. Poljak¹⁰¹, A. Pop⁴⁹, S. Porteboeuf-Houssais¹³⁶, J. Porter⁸¹, V. Pozdniakov⁷⁶, S.K. Prasad⁴, R. Preghenella⁵⁵, F. Prino⁶⁰, C.A. Pruneau¹⁴⁴, I. Pshenichnov⁶⁴, M. Puccio³⁵, S. Qiu⁹², L. Quaglia²⁵, R.E. Quishpe¹²⁶, S. Ragoni¹¹², A. Rakotozafindrabe¹³⁹, L. Ramello³², F. Rami¹³⁸, S.A.R. Ramirez⁴⁶, A.G.T. Ramos³⁴, R. Raniwala¹⁰⁴, S. Raniwala¹⁰⁴, S.S. Räsänen⁴⁵, R. Rath⁵¹, I. Ravasenga⁹², K.F. Read^{98,132}, A.R. Redelbach⁴⁰, K. Redlich^{87,V}, A. Rehman²¹, P. Reichelt⁶⁹, F. Reidt³⁵, H.A. Reme-ness³⁷, R. Renfordt⁶⁹, Z. Rescakova³⁹, K. Reygers¹⁰⁶, A. Riabov¹⁰⁰, V. Riabov¹⁰⁰, T. Richert^{82,91}, M. Richter²⁰, W. Riegler³⁵, F. Riggi²⁷, C. Ristea⁶⁸, S.P. Rode⁵¹, M. Rodríguez Cahuantzi⁴⁶, K. Røed²⁰, R. Rogalev⁹³, E. Rogochaya⁷⁶, T.S. Rogoschinski⁶⁹, D. Rohr³⁵, D. Röhrich²¹, P.F. Rojas⁴⁶, P.S. Rokita¹⁴³, F. Ronchetti⁵³, A. Rosano^{33,57},

E.D. Rosas⁷⁰, A. Rossi⁵⁸, A. Rotondi²⁹, A. Roy⁵¹, P. Roy¹¹¹, S. Roy⁵⁰, N. Rubini²⁶, O.V. Rueda⁸², R. Rui²⁴, B. Rumyantsev⁷⁶, A. Rustamov⁸⁹, E. Ryabinkin⁹⁰, Y. Ryabov¹⁰⁰, A. Rybicki¹¹⁹, H. Ryttonen¹²⁷, W. Rzeska¹⁴³, O.A.M. Saarimaki⁴⁵, R. Sadek¹¹⁶, S. Sadovsky⁹³, J. Saetre²¹, K. Šafařík³⁸, S.K. Saha¹⁴², S. Saha⁸⁸, B. Sahoo⁵⁰, P. Sahoo⁵⁰, R. Sahoo⁵¹, S. Sahoo⁶⁶, D. Sahu⁵¹, P.K. Sahu⁶⁶, J. Saini¹⁴², S. Sakai¹³⁵, S. Sambyal¹⁰³, V. Samsonov^{100,95,1}, D. Sarkar¹⁴⁴, N. Sarkar¹⁴², P. Sarma⁴³, V.M. Sarti¹⁰⁷, M.H.P. Sas¹⁴⁷, J. Schambach^{98,120}, H.S. Scheid⁶⁹, C. Schiaua⁴⁹, R. Schicker¹⁰⁶, A. Schmah¹⁰⁶, C. Schmidt¹⁰⁹, H.R. Schmidt¹⁰⁵, M.O. Schmidt¹⁰⁶, M. Schmidt¹⁰⁵, N.V. Schmidt^{98,69}, A.R. Schmier¹³², R. Schotter¹³⁸, J. Schukraft³⁵, Y. Schutz¹³⁸, K. Schwarz¹⁰⁹, K. Schweda¹⁰⁹, G. Scioli²⁶, E. Scomparin⁶⁰, J.E. Seger¹⁵, Y. Sekiguchi¹³⁴, D. Sekihata¹³⁴, I. Selyuzhenkov^{109,95}, S. Senyukov¹³⁸, J.J. Seo⁶², D. Serebryakov⁶⁴, L. Šerkšnytė¹⁰⁷, A. Sevcenco⁶⁸, T.J. Shaba⁷³, A. Shabanov⁶⁴, A. Shabetai¹¹⁶, R. Shahoyan³⁵, W. Shaikh¹¹¹, A. Shangaraev⁹³, A. Sharma¹⁰², H. Sharma¹¹⁹, M. Sharma¹⁰³, N. Sharma¹⁰², S. Sharma¹⁰³, O. Sheibani¹²⁶, K. Shigaki⁴⁷, M. Shimomura⁸⁵, S. Shirinkin⁹⁴, Q. Shou⁴¹, Y. Sibiriak⁹⁰, S. Siddhanta⁵⁶, T. Siemiarczuk⁸⁷, T.F. Silva¹²², D. Silvermyr⁸², G. Simonetti³⁵, B. Singh¹⁰⁷, R. Singh⁸⁸, R. Singh¹⁰³, R. Singh⁵¹, V.K. Singh¹⁴², V. Singhal¹⁴², T. Sinha¹¹¹, B. Sitar¹³, M. Sitta³², T.B. Skaali²⁰, G. Skorodumovs¹⁰⁶, M. Slupecki⁴⁵, N. Smirnov¹⁴⁷, R.J.M. Snellings⁶³, C. Soncco¹¹³, J. Song¹²⁶, A. Songmoolnak¹¹⁷, F. Soramel²⁸, S. Sorensen¹³², I. Sputowska¹¹⁹, J. Stachel¹⁰⁶, I. Stan⁶⁸, P.J. Steffanic¹³², S.F. Stiefelmaier¹⁰⁶, D. Stocco¹¹⁶, I. Storehaug²⁰, M.M. Støretvedt³⁷, C.P. Stylianidis⁹², A.A.P. Suaide¹²², T. Sugitate⁴⁷, C. Suire⁷⁹, M. Suljic³⁵, R. Sultanov⁹⁴, M. Šumbera⁹⁷, V. Sumberia¹⁰³, S. Sumowidagdo⁵², S. Swain⁶⁶, A. Szabo¹³, I. Szarka¹³, U. Tabassam¹⁴, S.F. Taghavi¹⁰⁷, G. Tallepied¹³⁶, J. Takahashi¹²³, G.J. Tambave²¹, S. Tang^{136,7}, Z. Tang¹³⁰, M. Tarhini¹¹⁶, M.G. Tarzila⁴⁹, A. Tauro³⁵, G. Tejada Muñoz⁴⁶, A. Telesca³⁵, L. Terlizzi²⁵, C. Terrevoli¹²⁶, G. Tersimonov³, S. Thakur¹⁴², D. Thomas¹²⁰, R. Tieulent¹³⁷, A. Tikhonov⁶⁴, A.R. Timmins¹²⁶, M. Tkacik¹¹⁸, A. Toia⁶⁹, N. Topilskaya⁶⁴, M. Toppi⁵³, F. Torres-Acosta¹⁹, S.R. Torres³⁸, A. Trifiró^{33,57}, S. Tripathy^{55,70}, T. Tripathy⁵⁰, S. Trogolo^{35,28}, G. Trombetta³⁴, V. Trubnikov³, W.H. Trzaska¹²⁷, T.P. Trzcinski¹⁴³, B.A. Trzeciak³⁸, A. Tumkin¹¹⁰, R. Turrisi⁵⁸, T.S. Tveter²⁰, K. Ullaland²¹, A. Uras¹³⁷, M. Urioni¹⁴¹, G.L. Usai²³, M. Vala³⁹, N. Valle²⁹, S. Vallero⁶⁰, N. van der Kolk⁶³, L.V.R. van Doremalen⁶³, M. van Leeuwen⁹², P. Vande Vyvre³⁵, D. Varga¹⁴⁶, Z. Varga¹⁴⁶, M. Varga-Kofarago¹⁴⁶, A. Vargas⁴⁶, M. Vasileiou⁸⁶, A. Vasiliev⁹⁰, O. Vázquez Doce¹⁰⁷, V. Vechernin¹¹⁴, E. Vercellin²⁵, S. Vergara Limón⁴⁶, L. Vermunt⁶³, R. Vértési¹⁴⁶, M. Verweij⁶³, L. Vickovic³⁶, Z. Vilakazi¹³³, O. Villalobos Baillie¹¹², G. Vino⁵⁴, A. Vinogradov⁹⁰, T. Virgili³⁰, V. Vislavicius⁹¹, A. Vodopyanov⁷⁶, B. Volkel³⁵, M.A. Völkl¹⁰⁶, K. Voloshin⁹⁴, S.A. Voloshin¹⁴⁴, G. Volpe³⁴, B. von Haller³⁵, I. Vorobyev¹⁰⁷, D. Voscek¹¹⁸, J. Vrláková³⁹, B. Wagner²¹, C. Wang⁴¹, D. Wang⁴¹, M. Weber¹¹⁵, A. Wegrzynek³⁵, S.C. Wenzel³⁵, J.P. Wessels¹⁴⁵, J. Wiechula⁶⁹, J. Wikne²⁰, G. Wilk⁸⁷, J. Wilkinson¹⁰⁹, G.A. Willems¹⁴⁵, E. Willsher¹¹², B. Windelband¹⁰⁶, M. Winn¹³⁹, W.E. Witt¹³², J.R. Wright¹²⁰, W. Wu⁴¹, Y. Wu¹³⁰, R. Xu⁷, S. Yalcin⁷⁸, Y. Yamaguchi⁴⁷, K. Yamakawa⁴⁷, S. Yang²¹, S. Yano^{47,139}, Z. Yin⁷, H. Yokoyama⁶³, I.-K. Yoo¹⁷, J.H. Yoon⁶², S. Yuan²¹, A. Yuncu¹⁰⁶, V. Zaccaro²⁴, A. Zaman¹⁴, C. Zampolli³⁵, H.J.C. Zanoli⁶³, N. Zardoshti³⁵, A. Zarochentsev¹¹⁴, P. Závada⁶⁷, N. Zaviyalov¹¹⁰, H. Zbroszczyk¹⁴³, M. Zhalov¹⁰⁰, S. Zhang⁴¹, X. Zhang⁷, Y. Zhang¹³⁰, V. Zhrebchevskii¹¹⁴, Y. Zhi¹¹, D. Zhou⁷, Y. Zhou⁹¹, J. Zhu^{7,109}, A. Zichichi²⁶, G. Zinovjev³, N. Zurlo¹⁴¹

¹ A.I. Alikhanyan National Science Laboratory (Yerevan Physics Institute) Foundation, Yerevan, Armenia

² AGH University of Science and Technology, Cracow, Poland

³ Bogolyubov Institute for Theoretical Physics, National Academy of Sciences of Ukraine, Kiev, Ukraine

⁴ Bose Institute, Department of Physics and Centre for Astroparticle Physics and Space Science (CAPSS), Kolkata, India

⁵ Budker Institute for Nuclear Physics, Novosibirsk, Russia

⁶ California Polytechnic State University, San Luis Obispo, CA, United States

⁷ Central China Normal University, Wuhan, China

⁸ Centro de Aplicaciones Tecnológicas y Desarrollo Nuclear (CEADEN), Havana, Cuba

⁹ Centro de Investigación y de Estudios Avanzados (CINVESTAV), Mexico City and Mérida, Mexico

¹⁰ Chicago State University, Chicago, IL, United States

¹¹ China Institute of Atomic Energy, Beijing, China

¹² Chungbuk National University, Cheongju, Republic of Korea

¹³ Comenius University Bratislava, Faculty of Mathematics, Physics and Informatics, Bratislava, Slovakia

¹⁴ COMSATS University Islamabad, Islamabad, Pakistan

¹⁵ Creighton University, Omaha, NE, United States

¹⁶ Department of Physics, Aligarh Muslim University, Aligarh, India

¹⁷ Department of Physics, Pusan National University, Pusan, Republic of Korea

¹⁸ Department of Physics, Sejong University, Seoul, Republic of Korea

¹⁹ Department of Physics, University of California, Berkeley, CA, United States

²⁰ Department of Physics, University of Oslo, Oslo, Norway

²¹ Department of Physics and Technology, University of Bergen, Bergen, Norway

- 22 Dipartimento di Fisica dell'Università 'La Sapienza' and Sezione INFN, Rome, Italy
 23 Dipartimento di Fisica dell'Università and Sezione INFN, Cagliari, Italy
 24 Dipartimento di Fisica dell'Università and Sezione INFN, Trieste, Italy
 25 Dipartimento di Fisica dell'Università and Sezione INFN, Turin, Italy
 26 Dipartimento di Fisica e Astronomia dell'Università and Sezione INFN, Bologna, Italy
 27 Dipartimento di Fisica e Astronomia dell'Università and Sezione INFN, Catania, Italy
 28 Dipartimento di Fisica e Astronomia dell'Università and Sezione INFN, Padova, Italy
 29 Dipartimento di Fisica e Nucleare e Teorica, Università di Pavia, Pavia, Italy
 30 Dipartimento di Fisica 'E.R. Caianiello' dell'Università and Gruppo Collegato INFN, Salerno, Italy
 31 Dipartimento DISAT del Politecnico and Sezione INFN, Turin, Italy
 32 Dipartimento di Scienze e Innovazione Tecnologica dell'Università del Piemonte Orientale and INFN Sezione di Torino, Alessandria, Italy
 33 Dipartimento di Scienze MIFT, Università di Messina, Messina, Italy
 34 Dipartimento Interateneo di Fisica 'M. Merlin' and Sezione INFN, Bari, Italy
 35 European Organization for Nuclear Research (CERN), Geneva, Switzerland
 36 Faculty of Electrical Engineering, Mechanical Engineering and Naval Architecture, University of Split, Split, Croatia
 37 Faculty of Engineering and Science, Western Norway University of Applied Sciences, Bergen, Norway
 38 Faculty of Nuclear Sciences and Physical Engineering, Czech Technical University in Prague, Prague, Czech Republic
 39 Faculty of Science, P.J. Šafárik University, Košice, Slovakia
 40 Frankfurt Institute for Advanced Studies, Johann Wolfgang Goethe-Universität Frankfurt, Frankfurt, Germany
 41 Fudan University, Shanghai, China
 42 Gangneung-Wonju National University, Gangneung, Republic of Korea
 43 Gauhati University, Department of Physics, Guwahati, India
 44 Helmholtz-Institut für Strahlen- und Kernphysik, Rheinische Friedrich-Wilhelms-Universität Bonn, Bonn, Germany
 45 Helsinki Institute of Physics (HIP), Helsinki, Finland
 46 High Energy Physics Group, Universidad Autónoma de Puebla, Puebla, Mexico
 47 Hiroshima University, Hiroshima, Japan
 48 Hochschule Worms, Zentrum für Technologietransfer und Telekommunikation (ZTT), Worms, Germany
 49 Horia Hulubei National Institute of Physics and Nuclear Engineering, Bucharest, Romania
 50 Indian Institute of Technology Bombay (IIT), Mumbai, India
 51 Indian Institute of Technology Indore, Indore, India
 52 Indonesian Institute of Sciences, Jakarta, Indonesia
 53 INFN, Laboratori Nazionali di Frascati, Frascati, Italy
 54 INFN, Sezione di Bari, Bari, Italy
 55 INFN, Sezione di Bologna, Bologna, Italy
 56 INFN, Sezione di Cagliari, Cagliari, Italy
 57 INFN, Sezione di Catania, Catania, Italy
 58 INFN, Sezione di Padova, Padova, Italy
 59 INFN, Sezione di Roma, Rome, Italy
 60 INFN, Sezione di Torino, Turin, Italy
 61 INFN, Sezione di Trieste, Trieste, Italy
 62 Inha University, Incheon, Republic of Korea
 63 Institute for Gravitational and Subatomic Physics (GRASP), Utrecht University/Nikhef, Utrecht, Netherlands
 64 Institute for Nuclear Research, Academy of Sciences, Moscow, Russia
 65 Institute of Experimental Physics, Slovak Academy of Sciences, Košice, Slovakia
 66 Institute of Physics, Homi Bhabha National Institute, Bhubaneswar, India
 67 Institute of Physics of the Czech Academy of Sciences, Prague, Czech Republic
 68 Institute of Space Science (ISS), Bucharest, Romania
 69 Institut für Kernphysik, Johann Wolfgang Goethe-Universität Frankfurt, Frankfurt, Germany
 70 Instituto de Ciencias Nucleares, Universidad Nacional Autónoma de México, Mexico City, Mexico
 71 Instituto de Física, Universidade Federal do Rio Grande do Sul (UFRGS), Porto Alegre, Brazil
 72 Instituto de Física, Universidad Nacional Autónoma de México, Mexico City, Mexico
 73 iThemba LABS, National Research Foundation, Somerset West, South Africa
 74 Jeonbuk National University, Jeonju, Republic of Korea
 75 Johann-Wolfgang-Goethe Universität Frankfurt Institut für Informatik, Fachbereich Informatik und Mathematik, Frankfurt, Germany
 76 Joint Institute for Nuclear Research (JINR), Dubna, Russia
 77 Korea Institute of Science and Technology Information, Daejeon, Republic of Korea
 78 KTO Karatay University, Konya, Turkey
 79 Laboratoire de Physique des 2 Infinis, Irène Joliot-Curie, Orsay, France
 80 Laboratoire de Physique Subatomique et de Cosmologie, Université Grenoble-Alpes, CNRS-IN2P3, Grenoble, France
 81 Lawrence Berkeley National Laboratory, Berkeley, CA, United States
 82 Lund University Department of Physics, Division of Particle Physics, Lund, Sweden
 83 Moscow Institute for Physics and Technology, Moscow, Russia
 84 Nagasaki Institute of Applied Science, Nagasaki, Japan
 85 Nara Women's University (NWU), Nara, Japan
 86 National and Kapodistrian University of Athens, School of Science, Department of Physics, Athens, Greece
 87 National Centre for Nuclear Research, Warsaw, Poland
 88 National Institute of Science Education and Research, Homi Bhabha National Institute, Jatni, India
 89 National Nuclear Research Center, Baku, Azerbaijan
 90 National Research Centre Kurchatov Institute, Moscow, Russia
 91 Niels Bohr Institute, University of Copenhagen, Copenhagen, Denmark
 92 Nikhef, National Institute for Subatomic Physics, Amsterdam, Netherlands
 93 NRC Kurchatov Institute IHEP, Protvino, Russia
 94 NRC «Kurchatov» Institute – ITEP, Moscow, Russia
 95 NRNU Moscow Engineering Physics Institute, Moscow, Russia
 96 Nuclear Physics Group, STFC Daresbury Laboratory, Daresbury, United Kingdom
 97 Nuclear Physics Institute of the Czech Academy of Sciences, Řež u Prahy, Czech Republic
 98 Oak Ridge National Laboratory, Oak Ridge, TN, United States
 99 Ohio State University, Columbus, OH, United States
 100 Petersburg Nuclear Physics Institute, Gatchina, Russia
 101 Physics Department, Faculty of Science, University of Zagreb, Zagreb, Croatia

- 102 Physics Department, Panjab University, Chandigarh, India
 103 Physics Department, University of Jammu, Jammu, India
 104 Physics Department, University of Rajasthan, Jaipur, India
 105 Physikalisches Institut, Eberhard-Karls-Universität Tübingen, Tübingen, Germany
 106 Physikalisches Institut, Ruprecht-Karls-Universität Heidelberg, Heidelberg, Germany
 107 Physik Department, Technische Universität München, Munich, Germany
 108 Politecnico di Bari and Sezione INFN, Bari, Italy
 109 Research Division and ExtreMe Matter Institute EMMI, GSI Helmholtzzentrum für Schwerionenforschung GmbH, Darmstadt, Germany
 110 Russian Federal Nuclear Center (VNIIEF), Sarov, Russia
 111 Saha Institute of Nuclear Physics, Homi Bhabha National Institute, Kolkata, India
 112 School of Physics and Astronomy, University of Birmingham, Birmingham, United Kingdom
 113 Sección Física, Departamento de Ciencias, Pontificia Universidad Católica del Perú, Lima, Peru
 114 St. Petersburg State University, St. Petersburg, Russia
 115 Stefan Meyer Institut für Subatomare Physik (SMI), Vienna, Austria
 116 SUBATECH, IMT Atlantique, Université de Nantes, CNRS-IN2P3, Nantes, France
 117 Suranaree University of Technology, Nakhon Ratchasima, Thailand
 118 Technical University of Košice, Košice, Slovakia
 119 The Henryk Niewodniczanski Institute of Nuclear Physics, Polish Academy of Sciences, Cracow, Poland
 120 The University of Texas at Austin, Austin, TX, United States
 121 Universidad Autónoma de Sinaloa, Culiacán, Mexico
 122 Universidade de São Paulo (USP), São Paulo, Brazil
 123 Universidade Estadual de Campinas (UNICAMP), Campinas, Brazil
 124 Universidade Federal do ABC, Santo Andre, Brazil
 125 University of Cape Town, Cape Town, South Africa
 126 University of Houston, Houston, TX, United States
 127 University of Jyväskylä, Jyväskylä, Finland
 128 University of Kansas, Lawrence, KS, United States
 129 University of Liverpool, Liverpool, United Kingdom
 130 University of Science and Technology of China, Hefei, China
 131 University of South-Eastern Norway, Tonsberg, Norway
 132 University of Tennessee, Knoxville, TN, United States
 133 University of the Witwatersrand, Johannesburg, South Africa
 134 University of Tokyo, Tokyo, Japan
 135 University of Tsukuba, Tsukuba, Japan
 136 Université Clermont Auvergne, CNRS/IN2P3, LPC, Clermont-Ferrand, France
 137 Université de Lyon, CNRS/IN2P3, Institut de Physique des 2 Infinis de Lyon, Lyon, France
 138 Université de Strasbourg, CNRS, IPHC UMR 7178, F-67000 Strasbourg, France
 139 Université Paris-Saclay Centre d'Etudes de Saclay (CEA), IRFU, Département de Physique Nucléaire (DPhN), Saclay, France
 140 Università degli Studi di Foggia, Foggia, Italy
 141 Università di Brescia, Brescia, Italy
 142 Variable Energy Cyclotron Centre, Homi Bhabha National Institute, Kolkata, India
 143 Warsaw University of Technology, Warsaw, Poland
 144 Wayne State University, Detroit, MI, United States
 145 Westfälische Wilhelms-Universität Münster, Institut für Kernphysik, Münster, Germany
 146 Wigner Research Centre for Physics, Budapest, Hungary
 147 Yale University, New Haven, CT, United States
 148 Yonsei University, Seoul, Republic of Korea

^I Deceased.

^{II} Also at: Italian National Agency for New Technologies, Energy and Sustainable Economic Development (ENEA), Bologna, Italy.

^{III} Also at: Dipartimento DET del Politecnico di Torino, Turin, Italy.

^{IV} Also at: M.V. Lomonosov Moscow State University, D.V. Skobeltsyn Institute of Nuclear, Physics, Moscow, Russia.

^V Also at: Institute of Theoretical Physics, University of Wrocław, Poland.